Detachment of Deposited Colloids by Advancing and Receding Air–Water Interfaces

ARTICLE *in* LANGMUIR · JUNE 2011

Impact Factor: 4.46 · DOI: 10.1021/la201840q · Source: PubMed

3 AUTHORS, INCLUDING:

James B Harsh
Washington State University
90 PUBLICATIONS **1,708** CITATIONS

SEE PROFILE

Langmuir

ARTICLE

pubs.acs.org/Langmuir

Detachment of Deposited Colloids by Advancing and Receding Air−Water Interfaces

Surachet Aramrak,[†] Markus Flury,[*,†,‡] and James B. Harsh[†]

[†]Department of Crop and Soil Sciences, Washington State University, Pullman, Washington 99164, United States

[‡]Department of Crop and Soil Sciences, Washington State University, Puyallup, Washington 98371, United States

Supporting Information

ABSTRACT: Moving air−water interfaces can detach colloidal particles from stationary surfaces. The objective of this study was to quantify the effects of advancing and receding air−water interfaces on colloid detachment as a function of interface velocity. We deposited fluorescent, negatively charged, carboxylate-modified polystyrene colloids (diameter of 1 μm) into a cylindrical glass channel. The colloids were hydrophilic with an advancing air−water contact angle of 60° and a receding contact angle of 40°. After colloid deposition, two air bubbles were sequentially introduced into the glass channel and passed through the channel at different velocities (0.5, 7.7, 72, 982, and 10 800 cm/h). The passage of the bubbles represented a sequence of receding and advancing air−water interfaces. Colloids remaining in the glass channel after each interface passage were visualized with confocal microscopy and quantified by image analysis. The advancing air−water interface was significantly more effective in detaching colloids from the glass surface than the receding interface. Most of the colloids were detached during the first passage of the advancing air−water interface, while the subsequent interface passages did not remove significant amounts of colloids. Forces acting on the colloids calculated from theory corroborate our experimental results, and confirm that the detachment forces (surface tension forces) during the advancing air−water interface movement were stronger than during the receding movement. Theory indicates that, for hydrophilic colloids, the advancing interface movement generally exerts a stronger detachment force than the receding, except when the hysteresis of the colloid-air−water contact angle is small and that of the channel-air−water contact angle is large.

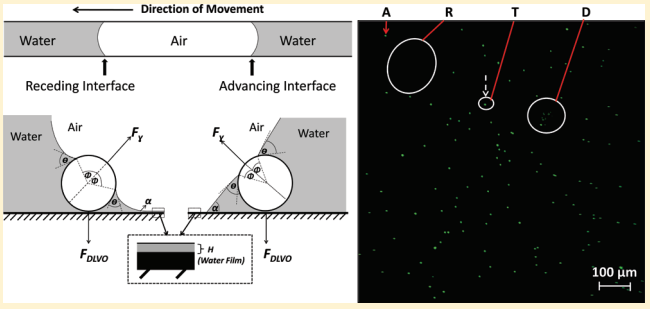

1. INTRODUCTION

One of the most striking phenomena in nature related to particle−air−water interface interactions is the rolling of water droplets on Lotus leaves.[1,2] Due to the hydrophobic surface of Lotus leaves, water droplets roll off the slanted leaf, and as they roll downward driven by gravity, dust particles are removed from the leaf surface, resulting in a self-cleaning process, called the "Lotus-Effect".[2−4] The removal of dust particles is due to attachment of the particles to the air−water interface.[3,5] This self-cleaning process observed with Lotus leaves has several industrial parallels, including cleaning of wafers in microelectronics.[6] One of the most prominent examples of an industrial application of particle−air−water interface attachment is froth flotation, used in the mining industry to separate different minerals based on the preferential attachment to gas bubbles.[7,8]

Moving air−water interfaces also occur in geologic media, i.e., the unsaturated subsurface or the vadose zone. The unsaturated subsurface is a three-phase system, consisting of air, water, and solid phases, and air−water interfaces move when water infiltrates or drains from the system. Such infiltration and drainage events occur frequently in nature during rainfall events. It has been reported that infiltration fronts can mobilize substantial amounts of particles from sediments or soils.[9−11] Particles themselves can be contaminants or can associate with contaminants, thereby providing a pathway for contaminant transport.[12−14] Thus, the interaction of particles and moving air−water interfaces is an important process in subsurface systems with regard to environmental protection.

Particles attached to the air−water interface experience strong capillary forces.[15−17] These forces can exceed solid−water adhesion forces by several orders of magnitude,[10,18] and this is the basis for dust and colloid removal by moving air−water interfaces used in microelectronics.[5,6] Several mechanistic studies on how moving air−water interfaces can be used to remove colloidal particles from a solid surface have been reported.[6,18−22] In these studies, colloids were deposited on the inner surface of a parallel plate flow chamber[6,18,19,21,22] or onto a microscopy slide,[23] and then removed by passing air−water interfaces over the deposited colloids. The results showed that colloid detachment by the air−water interface was more effective when colloids

Received: May 16, 2011
Revised: June 28, 2011
Published: June 29, 2011

were deposited under unfavorable as compared to favorable conditions,[21,23] when the velocity of the air−water interface decreased,[21,23] when colloidal size increased,[22] when colloids were hydrophobic as opposed to hydrophilic,[23] and when the air−liquid surface tension increased.[21]

Experimental evidence indicates that, while colloid detachment by a moving air−water interface generally increases with decreasing interface velocity, the sensitivity of detachment to interface velocity is stronger the larger and more hydrophobic the colloids are.[22] A linear relationship between the air−water interface velocity and the amount of colloid detachment was observed for velocities in the range of 700 to 5000 cm/h;[21] however, at lower interface velocities of 0.4 to 400 cm/h, Sharma et al.[23] found no linear relationship, yet the general trend of decreasing detachment with increasing velocity was confirmed. Detachment of colloids with opposite charge to the collector surface was more sensitive to interface velocity as compared to detachment of colloids deposited on a like-charged collector surface.[21,23]

The effect of moving air−water interfaces on the detachment of colloidal particles from both initially wet solid surfaces[6,18,19,21,22] and initially air-dried surfaces[23] has been investigated under different physical and chemical conditions. Both initially wet and dry conditions occur often in nature. In the subsurface, the air−water interface passes over initially air-dried surfaces when water infiltrates or imbibes dry soils or sediments, while the interface passes over initially wet surfaces when water imbibes into moist soil or when drainage occurs. Column-scale experiments with porous media have shown that colloidal particles are mobilized from sediments during infiltration and drainage events,[9,24−26] and it has indeed been demonstrated that the air−water interface is contributing considerably to the mobilization.[11]

The interaction force between the air−water interface and a particle depends on the air−water−solid contact angle, for both the particle and the collector surface.[18] As advancing and receding interfaces have different contact angles with respect to particle and collector surface, the detachment force will be different as well.[16,20] Gomez-Suarez et al.[19] showed theoretically that detachment forces are larger for advancing than receding interfaces, but no experimental evidence has been reported from microscopic-scale experiments so far.

Our objective was to experimentally test the effect of advancing and receding air−water interfaces on detachment of colloidal particles from a solid surface. We used microscopic visualization to quantify colloid detachment from a hydrophilic glass surface by a sequence of advancing and receding air−water interfaces as a function of interface velocity.

2. EXPERIMENTAL SECTION

Approach. Our general experimental approach was to deposit colloidal particles onto a glass surface and then expose the deposited colloids to successive air−water interface passages. As the air−water interface moved over the deposited colloids, we quantified the colloid removal by using confocal microscopy and image analysis. Air−water interfaces were generated by inserting air bubbles into a water-filled capillary tube. Displacement experiments were carried out with in situ confocal microcopy so that we could differentiate between advancing and receding interfaces. All experiments were conducted at ambient temperature (18 to 20 °C). Figure 1 shows a schematic of the experimental setup.

Glass Channel Design. A cylindrical channel (3.7 mm inner diameter and 7.5 cm length) made of soda-lime glass was used as a surrogate for a pore channel. We cleaned the channel by first using compressed air to blow out dust (using a cleaning duster), then soaking in 99% acetone for 20 min, rinsing with 95% ethanol, scouring with an ethanol wet cotton swab, rinsing again with ethanol, followed by rinsing with double-deionized water. The rinsing procedures were repeated five times. The channel was finally dried at room temperature. Two 1-cm-long sections of a sterile stainless steel hypodermic needle (1.2 mm diameter, Monoject 250, Tyco) were glued with epoxy (General Purpose Epoxy, PermaPoxy, Permatex Inc., Solon, OH) to both sides of the channel. A small piece of a 6-mm-diameter glass rod with inner diameter of 1.5 mm was used to provide end-piece support for the needle tube. Two rectangularly shaped (25 mm × 10 mm) microscopy glass slides were glued to both ends of the channel to provide a support platform.

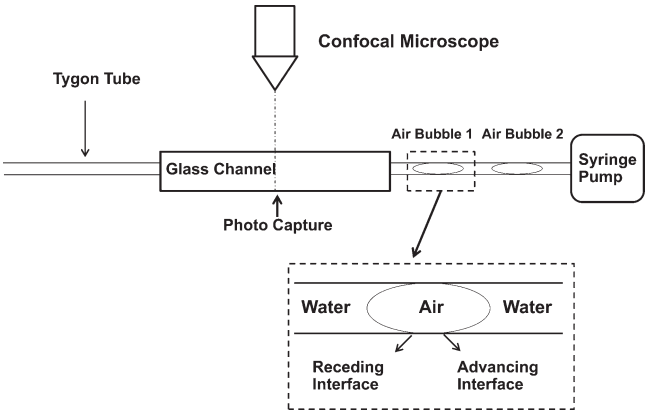

Figure 1. Schematic of experimental setup for air−water interface displacement.

Colloids and Suspension Chemistry. Hydrophilic carboxylate-modified microspheres (FluoSpheres, lot number 28120W, Molecular Probes, Inc., Eugene, OR) were selected as the colloid models in our experiment. The microspheres were negatively charged, fluorescent with an excitation/emission wavelength of 505/515 nm (yellow−green), had a diameter of 1.0 μm, a specific density of 1.055 g/cm^3, and surface charge of 0.0175 mol$_c$/g (Molecular Probes, Inc., Eugene, OR).

We intended to deposit colloids onto the inner surface of the glass channel as single, nonaggregated particles under nonfavorable conditions. We first tested solutions with different chemistry and used DLVO (Derjaguin−Landau−Verwey−Overbeek) calculations to optimize unfavorable attachment conditions. We first determined electrophoretic mobilities and ζ-potentials of the colloids and the channel at different pH values. For the glass channel, we ground the glass channel with a mortar to a fine powder and we then suspended the powder in aqueous solution. Electrophoretic mobilities were measured by dynamic light scattering (ZetaSizer 3000HSa, Malvern Instruments Ltd., Malvern, UK). All measurements were made in a solution of 1 mM $CaCl_2$ at different pH. Zeta potentials were derived from electrophoretic mobilities using the von Smoluchowski equation.[27] Using the measured zeta potentials, we then selected the pH value for the suspension that resulted in nonfavorable attachment conditions, i.e., where the DVLO profile showed a secondary energy minimum. The selected solution had pH 4.7 and 1 mM $CaCl_2$.

Characterization of Surface Properties of Glass Channel and Colloids. We determined advancing and receding air−liquid−solid contact angles with the tangent method by using a digital goniometer (DSA 100, Krüss, Hamburg, Germany). The liquid phase for these measurements was the aqueous solution determined above (1 mM $CaCl_2$ and pH 4.7). For the glass channel, we used a soda-lime microscopy slide (25 mm × 75 mm, Fisher brand, Fisher Scientific) as a surrogate. The slide was cleaned in the same manner as the glass channel described above. For colloids, a drop of a diluted microsphere

Table 1. Surface Properties of Colloids and Glass Channel (Soda-Lime Glass) (in 1 mM $CaCl_2$ and pH 4.7)

materials	contact angle (deg) advancing	contact angle (deg) receding	electrophoretic mobility (μm/s)(V/cm)	ζ-potential (mV)
carboxylate-modified microspheres	60.1 ± 3.0	39.7 ± 1.0	−3.01 ± 0.02	−38.3 ± 0.3
glass channel	27.2 ± 1.6	20.4 ± 2.9	−1.93 ± 0.05	−24.6 ± 0.7

suspension (0.5% by weight) was evaporated on a double-sided tape attached to the microscopy slide in a laminar flow chamber. This produced a uniform layer of colloids on the slide. For the contact angle measurements, we continuously dosed liquid onto the solid surface (either glass or colloids) at a rate of 5 μL/min and used a final drop size of 12 μL, following the procedures described by Shang et al.[28] The measured contact angles are macroscopic contact angles, and may differ from microscopic angles.[29] Electrophoretic mobilities and zeta potentials were determined as described above. Table 1 shows the characterization data.

Deposition of Colloids. Colloids were deposited onto the inner surface of the glass channel by circulating a colloid suspension through the channel. The deposition suspension was 1 mM $CaCl_2$, pH 4.7, and had a colloid concentration of 3.6×10^{11} particles/L. The channel was connected to Tygon tubing and a peristaltic pump (Ismatec IP4, Glattburg, Switzerland). Before the colloid suspension was introduced, the channel system was preconditioned with deionized water and the colloid-free solution for 20 min each, using a flow rate of 20 mL/h (average velocity in the channel 186 cm/h). Channel outflow of the preconditioning solution was discarded. The colloidal suspension was sonicated in an ultrasonic water bath for 1 min and then introduced into the channel. The Erlenmeyer flask containing the colloid suspension, the pump, and the channel formed a closed loop where the channel outflow recirculated into the Erlenmeyer flask at a flow rate of 20 mL/h. The colloidal suspension was recirculated for 2 h.

After the deposition, the channel was flushed for 4 h with the colloid-free solution to remove unattached colloids from the channel. After this flushing, the flow was stopped, and the channel, including the Tygon tubing, was removed from the pump. To prevent potential dust contamination, the colloidal deposition experiments were done in a laminar air-flow chamber (Laminar Airflow Cabinets, NuAire Corp., Plymouth, MN). The channel was then transferred to a confocal microscope for the interface displacement experiments.

Visualization and Quantification of Colloids. We used confocal microscopy to visualize the colloidal particles deposited inside the channel. Confocal or phase-contrast microscopy allows visualization of single colloids and has been used extensively in air−water interface displacement experiments.[19,21,23,30] We used a laser scanning confocal microscope (Axiovert 200 M equipped with LSM 510 META, Carl Zeiss Jena GmbH, Germany) and focused the field of view at the bottom of the channel with a magnification of 10. This allowed us to identify individual colloids. We scanned a fixed area of 900 μm by 900 μm during the course of the interface displacement experiments. Scanning of one image lasted 15 s. The images were then analyzed by the *ImageJ* software[31] to quantify the number of colloids.

Air−Water Interface Displacement Experiments. For the air−water interface displacement experiments, we used a syringe pump (KDS 200, KD Scientific, USA) to control the flow rates. One of the Tygon tubes of the channel system was connected to the pump and colloid-free solution (1 mM $CaCl_2$, pH 4.7) was passed through the channel at a constant flow rate. The inflow Tygon tube was bent into a U-shape and filled half with the colloid-free solution, leaving the end portions of the tube air-filled. After connecting to the channel and the pump, we had two air bubbles trapped in the inflow tube (Figure 1). These two air bubbles moved through the glass channel and provided a sequence of receding and advancing interface displacements: receding-1, advancing-1, receding-2, and advancing-2. Scanning confocal microscopy images were recorded before and after each interface passage over the scanning area. One initial image was recorded before flow was started to check whether the solution without an air−water interface will remove colloids. In addition, we recorded a scanning image of the interface itself (which was only possible at the low flow rates due to the time required to acquire an image). Each experiment was repeated 12 times, using a new channel for each replicate, i.e., each replicate was a completely independent experiment.

To examine the effect of the air−water interface velocity on colloid detachment, we varied the velocities by using the syringe pump. Our target velocities were 1, 10, 100, 1000, and 10 000 cm/h, but we were not able to exactly obtain these values. The experimentally measured velocities were 0.5, 7.7, 72, 982, and 10 800 cm/h, respectively. Although these measured velocities did not exactly match our target velocities, they were of the same order of magnitude. In the following, we use the target velocities when discussing and presenting the results, but we use the measured velocities to represent the data in tables, in figures, and in calculations.

The lower interface velocities (1, 10, and 100 cm/h) in our experiment were in the range of those used by Sharma et al.[23] who used velocities from 0.4 to 400 cm/h, the medium velocities (1000 and 10 000 cm/h) were in the range of those used by Gomez-Suarez et al.[21] who showed velocities from 700 to 5000 cm/h. The velocities of 1000 and 10 000 cm/h are in the range of the velocities reported for Haines jumps,[32,33] which have velocities in the range of 1000 to 100 000 cm/h.[34,35] The velocities used in our experiments correspond to Reynolds numbers of 0.01 to 115, indicating that the flow inside the channel was laminar at all velocities used.

To check whether the colloids removed by the moving air−water interfaces were initially deposited in the secondary energy minimum (i.e., unfavorable condition) or primary energy minimum, we conducted another set of experiments by changing the solution chemistry. We first calculated an appropriate solution chemistry using DLVO theory to determine a solution that will cause the secondary minimum to disappear. On this basis, we expected that, by changing the solution chemistry to the no-attachment condition (0.1 mM $CaCl_2$, pH 4.7), all colloids deposited in the secondary energy minimum would be released even without passage of air−water interfaces. We deposited the colloids into the channel as described above and then changed the solution chemistry to 0.1 mM $CaCl_2$ and pH 4.7. Visualization and quantification of colloids deposited on the glass channel was done before and after changing the solution chemistry at all the specific velocities indicated above. In these experiments, no air−water interface was present. As shown in the Results and Discussion section below, no colloids were removed at 0.1 mM $CaCl_2$ and pH 4.7, and therefore, we repeated these experiments by lowering the ionic strengths to 0.01, 0.001, and 0.0001 mM $CaCl_2$. Experiments were replicated three times.

Determination of the Effect of the Bubble Size. The faster the velocity of the air−water interface was, the more difficult it was to capture the colloidal images with the confocal microscope. To ease this step, we increased the size of the air bubble, providing a longer time for taking the images. To test whether the size of the air bubble in the tubing and channel affected colloid detachment, we did a series of experiments with two different bubble sizes. Air bubbles of 0.26 mL (standard bubble size used in our experiments) and 0.94 mL were introduced into the channel, and interface displacement experiments were conducted at a

velocity of 100 cm/h. Colloid detachment was visualized and quantified as described above. For each bubble size, we used 12 replicates. We found that the bubble size did not affect the experimental results, and we therefore used the bigger air bubbles for the experiments at velocities of 1000 and 10 000 cm/h.

Data Analysis. The images of colloids captured by the confocal microscope were analyzed by using the *ImageJ* software. Besides counting the total number of particles on the images, we used the mode of subtraction between images before and after interface movements to locate colloids that have remained stationary, colloids that have changed location, and colloids that have been removed. We analyzed the detachment data, i.e., the percentages of colloids detached after the passages of advancing and receding air−water interfaces, by using a one-way ANOVA and Turkey pairwise comparison to determine statistical differences at the 99% confidence level.[36]

3. THEORETICAL CONSIDERATIONS

DLVO Forces. We calculated colloid−glass surface interaction energies and forces by using DLVO theory according to the approach presented in Sharma et al.[23] The DLVO forces were calculated by differentiating the energy profile with respect to distance. The DLVO profiles for our chosen solution chemistry (1 mM $CaCl_2$, pH 4.7) showed the existence of a weak secondary energy minimum, where colloids would attach under nonfavorable conditions. When we reduced the ionic strength (0.1 mM $CaCl_2$, pH 4.7), the secondary minimum disappeared.

Surface Tension Forces. If an air−water interface is in contact with a solid particle, the net force acting on the particle is the sum of gravity, buoyancy, and interfacial forces. For small particles (radius <500 μm), the gravity and buoyancy forces are negligible compared to the interfacial forces.[16,23,37,38] In our experiments, we used particles with radius of 0.5 μm, and consequently, the interfacial force is the dominant force. When an air−water interface is in contact with a particle, the surface tension (interfacial) force F_γ normal to the interface orientation can be calculated by[6,19]

$$F_\gamma = 2\pi R_p \gamma \sin\phi \sin(\theta - \phi) \quad (1)$$

where R_p is the radius of the particle, γ is the surface tension of water, ϕ is the filling angle, and θ is the contact angle of the air−water interface with the particle. To obtain the maximum surface tension force,[6] we can differentiate eq 1 and obtain the maximum force when $\phi = \theta/2$. In the case where the air−water interface is bounded to a solid interface at one end, like in case of an interface in a glass channel, the surface tension force vector is tilted because of the nonsymmetry caused by the air−water−solid contact angle α (Figure 2). The maximum surface tension force $F_{\gamma,\max}$ is then given by[18,23]

$$F_{\gamma,\max} = 2\pi R_p \gamma \sin^2\left(\frac{\theta}{2}\right) \cos\alpha \quad \alpha < 90°, \text{vertical component} \quad (2)$$

and

$$F_{\gamma,\max} = 2\pi R_p \gamma \sin^2\left(\frac{\theta}{2}\right) \sin\alpha \quad \alpha < 90°, \text{horizontal component} \quad (3)$$

where α is the contact angle of the air−water interface with the glass surface. Because the contact angles θ and α are hysteretic with respect to the direction of the interface movement, it follows

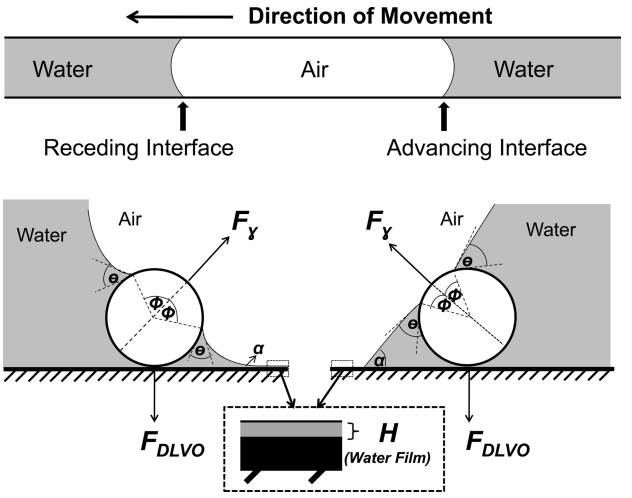

Figure 2. Schematic of surface tension force acting on a deposited colloid during receding and advancing air−water interface movement.

that the surface tension force will differ between advancing and receding interfaces. However, whether the surface tension force during advancing or receding interface movement is greater depends on the magnitude of the contact angle hysteresis and the absolute values of the contact angles.[18] In our experiments, the vertical component (eq 2) of the surface tension force acts against the adhesive DLVO force, resulting in lifting the deposited colloids up from the glass surface. The horizontal component (eq 3), on the other hand, will cause sliding and translocation of the deposited colloids over the glass surface.

Shear Force. In a dynamic system, when a moving air−water interface contacts a deposited particle, in addition to the surface tension force, a shear force acts on the particle. The shear force F_s can be expressed by[39]

$$F_s = 1.7(6\pi)\mu\left(\frac{H}{2}\right)V \quad (4)$$

where μ is the dynamic viscosity of water, H is the water film thickness, and V is the velocity of the liquid phase and the air−water interface. The shear force is maximal when the particle is completely exposed to the moving liquid, i.e., when $H/2 = R_p$.

Dynamic Thickness of Water Film. When an air bubble moves along with the fluid in a tube, a water film separates the air bubble from the tube wall; thus, the air−water interface does not make direct contact with the solid tube surface. Particles deposited on the tube surface generally will be detached by a moving air−water interface only if their diameters are larger than the water film thickness. For an air bubble moving in a tube, the thickness of the water film depends on the velocity of the air−water interface. Bretherton[40] approximated the film thickness H as function of the air bubble velocity V as

$$\frac{H}{w} = 0.643\left(\frac{3\mu V}{\gamma}\right)^{2/3} \quad (5)$$

where w is the diameter of the flow channel, μ is the dynamic viscosity, and γ is the surface tension. Equation 5 shows that increasing the velocity leads to an increased liquid-film thickness at the channel wall.

Contact and Induction Time during Colloid and Air−Water-Interface Interaction. Colloid attachment to the

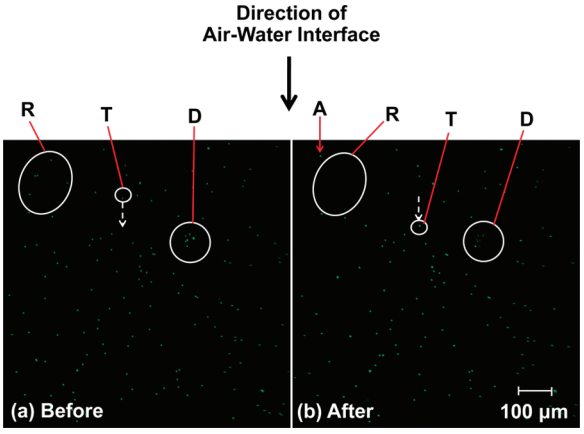

Figure 3. Modes of translocation of colloidal particles: (a) before and (b) after receding air−water interface passage. A: translocated into the field of view from upstream, R: removed from the solid surface, T: translocated to new position, and D: separated from colloid cluster. Images represent a fluid and interface velocity of 100 cm/h.

air−water interface is a time-dependent process, controlled by the contact time and the induction time.[41] The contact time t_c is the time of physical contact of the colloid with the air−water interface. The induction time t_i includes the times of thinning of the water film, the film rupture, and the formation of the air−water−solid interface line. Only colloids that contact the air−water interface for a time longer than the induction time will attach to the air−water interface. Thus, only if $t_c > t_i$ can attachment occur.[41]

In our experimental system, the contact time t_c can be estimated by

$$t_c = \frac{2R_p}{V} \tag{6}$$

where R_p is the colloid radius and V is the interface velocity. The induction time t_i can be calculated as[42]

$$t_i = \frac{3\mu R_f^2 R_p}{8m\gamma h_{cr}^2} \tag{7}$$

where R_f is the film radius, m is the mobility factor (1 for a completely retarded and 4 for a completely free bubble surface), and h_{cr} is the critical thickness of film rupture, which is given by[42]

$$h_{cr} = 23.3[\gamma(1 - \cos\theta_a)]^{0.16} \tag{8}$$

where h_{cr} has units of nm, the surface tension γ is in mN/m, and θ_a is the advancing contact angle.

The film radius R_f can be approximated by[42,43]

$$R_f = \frac{\pi R_p(656.9 - 87.4 \ln R_p)(Vt_{col})^{0.60}}{180} \tag{9}$$

where V is the air−water interface velocity, and t_{col} is the collision contact time.[42] In eq 9, the units are R_f (μm), V (cm/s), t_{col} (s).

The collision contact time can be calculated by[42]

$$t_{col} = \sqrt{\frac{\pi^2 R_p^3\left(\rho_p + 1.5\rho_{Fl}\right)}{3\gamma}} f \tag{10}$$

where ρ_p and ρ_{Fl} are the density of the particle and water, respectively, f is a nonlinear function depending on the properties of the particle and the surface tension of the fluid. We assumed that our f is equal to 5 according to Schulze.[42]

4. RESULTS AND DISCUSSION

Visualization and Modes of Colloid Translocation. We observed that the deposited colloids had different modes of translocation after the passage of an air−water interface. We illustrate the different modes for the passage of a receding interface at a velocity of 100 cm/h. Figure 3 shows the position of deposited colloids before (a) and after (b) passage of the air−water interface. The flow and the direction of the interface movement in the images are from top to bottom. Arrow A shows a colloidal particle that has moved into the image from upstream, i.e., has translocated into the field of view, either by sliding along the glass surface or by redeposition. Arrow R shows an area where colloids have been removed after the passage of the interface, while Arrow T shows a colloid that has apparently translocated along the direction of flow, likely by sliding along the glass surface. Arrow D shows a colloid cluster that has been broken up after passage of the air−water interface.

Figure 4 illustrates the general patterns observed during passages of an advancing and a receding air−water interface. The initial spatial distribution of the colloids on the glass surface (a) represents our reference from which we calculate colloid detachment. As the receding air−water interface moves over the field of view (b), more colloids are visible upstream of the interface, and we consider these colloids being attached at the thinning air−water interface trailing the interface front. We could identify the interface location optically because the colloids viewed through water and air phases had different brightness in the confocal microscope. After passage of the advancing air−water interface (c), we only see colloids remaining attached to the glass surface; compared with the initial amount of colloids, only a small fraction have been removed. The following advancing air−water interface showed a pronounced accumulation of colloids at the interface (d), and after passage of the interface, a large fraction of colloids have been removed from the glass surface.

Figure 5 shows an example of the sequence of images of the colloid distribution that we used for the quantitative data analysis for each set of experiments. The images represent the condition (a) before flow was started, (b) after flow was started but just before the air−water interface passed over the field of view, (c) after passage of the first receding interface, (d) after passage of the first advancing interface, (e) after passage of the second receding interface, and (f) after passage of the second advancing interface. It can be seen that (1) the flow itself without the passage of an air−water interface could not translocate or detach colloids from the glass surface (images a versus b); (2) the passage of the first receding interface did not remove as many colloids as did the first passage of the advancing interface (images c versus d); and (3) the passage of the second receding and second advancing interface was not causing substantial additional removal of colloids from the glass surface (images c through f). While these general patterns were observed in all our experiments, the quantitative magnitude of colloid translocations differed as a function of interface velocity as discussed below.

Colloid Attachment to the Glass Surface. The DLVO calculations indicated that the colloids attached to the glass surface under unfavorable conditions. However, the secondary energy minimum was too weak (∼ −0.1 kT) to keep colloids

dx.doi.org/10.1021/la201840q |*Langmuir* 2011, 27, 9985–9993

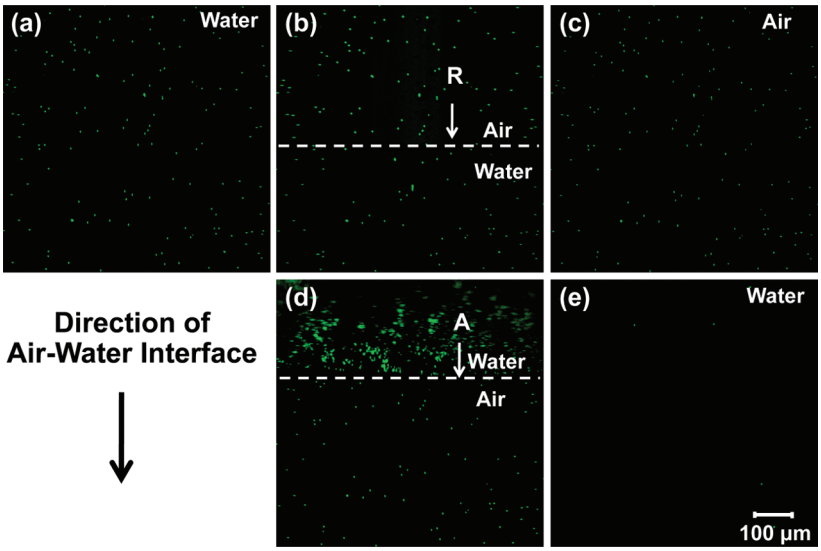

Figure 4. Detachment of deposited colloids from the solid surface by advancing and receding air−water interfaces: (a) initial condition, (b) during receding air−water interface movement, (c) after passage of receding air−water interface, (d) during advancing air−water interface movement, and (e) after passage of advancing air−water interface. R: position of receding air−water interface at the glass surface; A: position of the advancing air−water interface. Images represent a fluid and interface velocity of 100 cm/h.

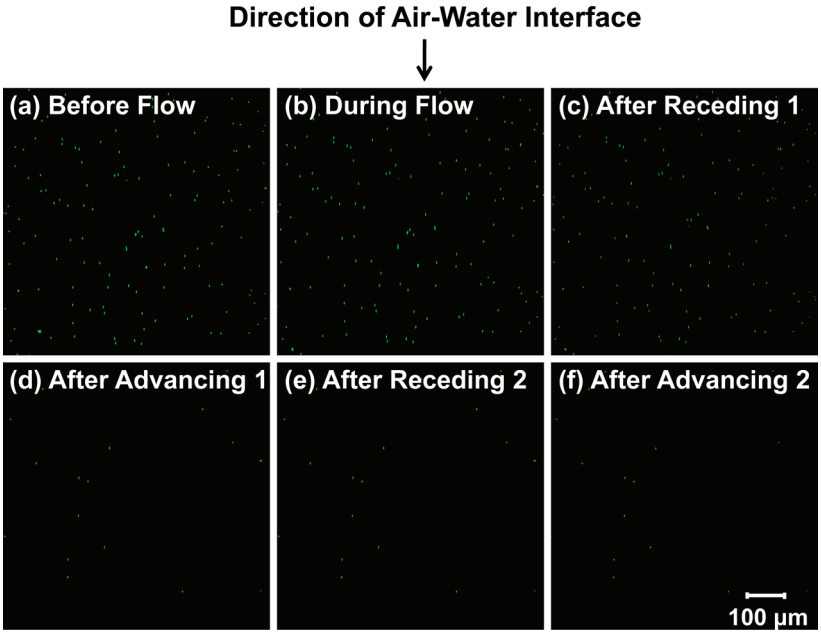

Figure 5. Detachment of deposited colloids after two successive air bubble movements: (a) initial condition before flow, (b) just before passage of the air−water interface, (c) after passage of first receding interface (receding-1), (d) after passage of first advancing interface (advancing-1), (e) after passage of second receding interface (receding-2), and (f) after passage of second advancing interface (advancing-2). Images represent a fluid and interface velocity of 100 cm/h.

attached. Our experiments showed that colloids remained attached to the glass surface after deposition and also after lowering the ionic strength to 0.1 mM $CaCl_2$. The colloids did not detach even after sequentially lowering the ionic strengths to 0.01, 0.001, and 0.0001 mM $CaCl_2$. We thus conclude that the attached colloids were all located in the primary energy minimum. It has been reported that chemical heterogeneities can cause differences in selectivity of attachment sites,[44,45] and local heterogeneities on glass surfaces can provide favorable attachment sites for negatively charged polystyrene colloids, particularly under low ionic strengths.[46] We assume that the distance between colloid and glass surface, when attached in the primary minimum, was 0.1 nm.[47]

Effect of Air−Water Interface Velocity on Colloid Detachment. Figure 6 and Table A (Supporting Information) show the quantitative amounts of colloids detached after passage of the air−water interfaces as a function of interface velocity. The percent detachment represents the number of colloids detached

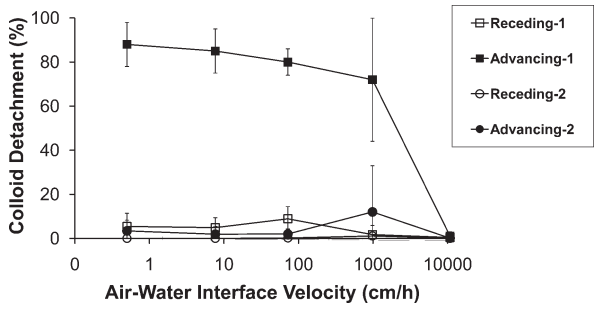

Figure 6. Detachment of deposited colloids as a function of air−water interface velocity. Solid symbols represent the advancing interface and open symbols represent receding interface. Symbols are arithmetic means and bars represent ± one standard deviation.

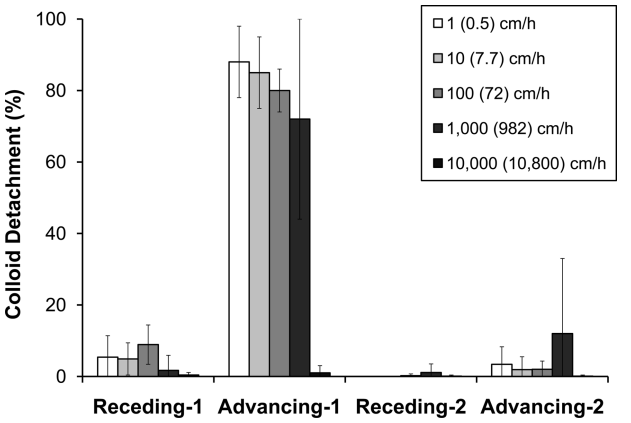

Figure 7. Percentage of colloid detachment for successive interface movements at different interface velocities. Bars are arithmetic means and lines represent ± one standard deviation. The numbers in parentheses are the measured velocities of the air−water interface.

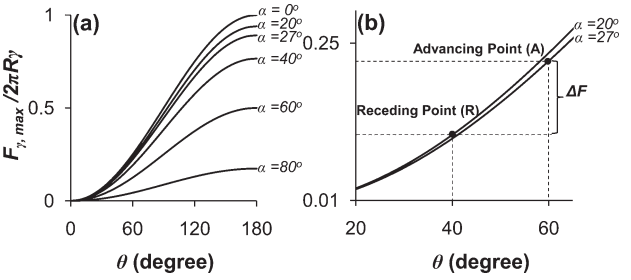

Figure 8. Maximum detachment force (eq 2, in dimensionless form ($F_{\gamma,\max}/(2\pi R\gamma)$) exerted by an air−water interface acting on a colloid deposited on glass-channel surface as a function of colloid−air−water contact angle (θ) and glass−air−water contact angle (α). (a) Full view, and (b) detailed view showing the regions of θ and α in our experiments (see Table 1).

by the respective air−water interface relative to the number of colloids just before the air−water interface has passed. The hydrodynamic force caused by the flow itself was not able to remove colloids from the glass surface at any velocity, as no colloids were removed during flow in absence of an air bubble (Table A, Supporting Information), and the surface tension force indeed was the dominant force causing colloid detachment. Colloid detachment was most pronounced at low flow velocities (1, 10, and 100 cm/h). The majority of the colloids were removed by the first advancing interface (advancing-1), and no significant difference in colloid detachment was observed among the three lowest velocities of 1, 10, and 100 cm/h. Indeed, for all interface passages, the amounts of colloids detached were not a function of interface velocities in the range of 1 to 100 cm/h; however, for faster velocities (1000 and 10 000 cm/h), colloid detachment drastically decreased. At a speed of 10 000 cm/h, no colloids were removed by any interface passage. While these general patterns were observed for all different interface passages, they were most pronounced for the first advancing interface (advancing-1).

Our data corroborate the results from Sharma et al.,[23] who observed the same velocity dependence of colloid detachment for carboxylate-modified polystyrene beads. Sharma et al.[23] operated with a narrower range of velocities and observed velocity-invariant detachment for velocities of 0.4, 0.8, 4, and 40 cm/h, but they observed decreased colloid detachment at an interface velocity of 400 cm/h. Gomez-Suarez et al.[20] found that colloid detachment from a quartz collector surface was dependent on interface velocity in the range of 700 to 5000 cm/h, with fewer colloids being detached as the velocity increased. Gomez-Suarez at al.[20] observed that less than 20% of colloids were detached by an air bubble (one receding and one advancing interface passage) at a velocity of 5000 cm/h. In our experiment, the detachment of colloids by the first air bubble (receding-1 and advancing-1) also decreased as the velocities increased from 100 to 1000 cm/h and was less than 1% at velocity of 10 000 cm/h (Figure 6). Our range of air−water interface velocities (1 to 10 000 cm/h) extends the ranges used in previous works, and our results and previous data indicate that the detachment of colloids significantly depends on the air−water interface velocity between 100 and 10 000 cm/h (Table A, Supporting Information).

Effect of the Sequence of Air−Water Interface Passage on Colloid Detachment. Here, we discuss the effect of the sequence of interface passages for velocities less than 100 cm/h, i.e., for velocities where colloid detachment was invariant of interface velocity. The first interface passage (receding-1) had only a small effect on colloid detachment: only about 5−10% of the attached colloids were detached (Figure 7). Most colloids were then detached by the first advancing interface passage (advancing-1) (80−88% (Figure 7). The subsequent second receding interface (receding-2) caused almost no further colloid detachment, while the second advancing interface (advancing-2) again detached significant, but small, amounts of colloids (2−3%).

Comparison of Experimental Results with Theory. With the exception of the 10 000 cm/h velocity, the advancing air−water interfaces were always more effective in detaching colloids than were the receding interfaces. On the basis of theory, it is indeed expected that the surface tension force causing detachment (eq 2) is larger for an advancing interface than for a receding interface for our experimental system. Figure 8a shows the maximum detachment force in dimensionless form as a function of the contact angles θ (colloid−air−water) and α (glass−air−water). The contact angles θ and α have opposite effects on the detachment force. This behavior is not because the surface tension force itself decreases with increasing α, but because the angle of the force vector changes (see Figure 2). Increasing α will decrease the vertical component of the surface tension vector.

Figure 8b shows a magnification of the area of interest for our experiments. At a receding contact angle $\theta = 40^o$ and $\alpha = 20^o$,

dx.doi.org/10.1021/la201840q |*Langmuir* 2011, 27, 9985–9993

Table 2. Forces Exerted on the Colloids during Passage of Advancing and Receding Air−Water Interfaces[a]

forces	receding air−water interface (μN)	advancing air−water interface (μN)
F_{DLVO} at 0.1 nm separation	3.14×10^{-2}	3.14×10^{-2}
$F_{\gamma,max}$ (vertical component)	2.49×10^{-2}	5.05×10^{-2}
$F_{\gamma,max}$ (horizontal component)	9.07×10^{-3}	2.58×10^{-2}
$F_{s,max}$ at 0.5 cm/h	1.99×10^{-8}	1.99×10^{-8}
$F_{s,max}$ at 7.7 cm/h	3.06×10^{-7}	3.06×10^{-7}
$F_{s,max}$ at 72 cm/h	2.87×10^{-6}	2.87×10^{-6}
$F_{s,max}$ at 982 cm/h	3.91×10^{-5}	3.91×10^{-5}
$F_{s,max}$ at 10 800 cm/h	4.30×10^{-4}	4.30×10^{-4}

[a] Forces were calculated with eqs 2, 3, and 4.

when the first interface passes over the colloids (point R), the dimensionless detachment force is $F_{\gamma,max}/(2\pi R\gamma) = 0.11$, but when the advancing interface passes (point A, where $\theta = 60^o$ and $\alpha = 27^o$), the detachment force increases to $F_{\gamma,max}/(2\pi R\gamma) = 0.22$, which constitutes an increase of 50%.

Table 2 summarizes the quantification of forces exerted on colloids during the passage of receding and advancing air−water interfaces. The DLVO and hydrodynamic forces, F_{DLVO} and $F_{s,max}$, are not a function of receding and advancing contact angles, and therefore are the same during receding and advancing events. For the vertical component of $F_{\gamma,max}$, which is opposite in direction to F_{DLVO}, the advancing $F_{\gamma,max}$ exceeded the F_{DLVO} by about 38% while the receding $F_{\gamma,max}$ was 21% less than F_{DLVO}. These force calculations corroborate our experimental results, i.e., most colloids were detached during passage of the advancing interface, but less than 1% during that of the receding interface (Figure 7). The horizontal component of $F_{\gamma,max}$ is smaller than F_{DLVO} and does not contribute to the detachment force because its direction is normal to F_{DLVO}. The hydrodynamic force $F_{s,max}$ increases linearly with air−water interface velocity, but was negligible relative to the other forces. Indeed, our experiments showed less than 1% colloid removal at the highest air−water interface velocity of 10 000 cm/h (Figure 6).

As the velocity increases, the water film thickness separating the air bubble from the channel wall increases (Figure 9). Depicted in Figure 9 are also the film thicknesses at our experimental velocities. At the three lowest velocities, the film thicknesses are all smaller than the colloid diameters, indicating that the colloids will form an air−water−solid interface with the air bubble. At a velocity of 1000 cm/h, the film thickness is larger than the colloid radius, but of similar magnitude, whereas at 10 000 cm/h, the film thickness is an order of magnitude larger than the colloid diameter. This suggests that at a velocity of 10 000 cm/h, there will be no air−water−colloid interface forming, and consequently, no colloids will be removed, as there exists no detaching surface tension force. This is corroborated by our experimental results. At a velocity 1000 cm/h, theoretically, no colloids should be removed either, but our experimental results show that colloids were removed. The amount of colloids removed was not as large as for the lower three velocities, but still,

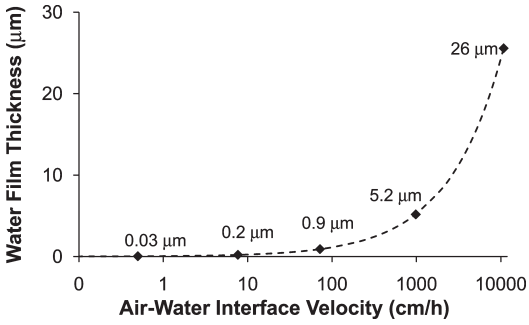

Figure 9. Water film thickness as a function of the velocity of the air−water interface. Dashed line is calculated with eq 5, symbols represent our experimental air−water interface velocities and the numbers show the corresponding water film thickness.

there was no significant difference in removal between the lower three and the 1000 cm/h velocity. We attribute this result to the fact that the colloid diameter and the film thickness at 1000 cm/h are of similar magnitude.

For colloids to be removed by an air−water interface, a colloid−air−water interface has to be formed. The critical time scales for this process are the contact time t_c and the induction time t_i (eqs 6 and 7). The contact times in our experiments were from 0.03 to 720 ms, depending on the interface velocity, whereas the induction times were on the order of 10^{-9} ms. Although the induction time, because of its empirical nature, may not be taken as an absolute value, it was several orders of magnitude smaller than the contact time, indicating that the film thinning, film rupture, and formation of the three-phase contact line was not a rate-limiting step. Overall, the theoretical calculations corroborate the experimental results, although the absolute calculations need to be considered approximate due to uncertainties in DLVO separation distances and contact angle measurements.

5. IMPLICATIONS

Moving air−water interfaces are of importance in many natural phenomena. Examples reach from sliding and rolling water droplets on leaves to the movement of water in porous media. The strong interaction of the air−water interface with colloids and particles has led to several industrial applications were moving air−water interfaces are used for colloid removal and particle separation.

Our results show the predominance of the advancing air−water interface movement over the receding interface movement on the detachment of deposited, hydrophilic colloids. Only in the special case where the colloid−air−water contact angle hysteresis is small compared to the channel−air−water contact angle hysteresis can the advancing interface movement become more dominant for hydrophilic colloids. On the basis of microscopic visualizations and pertinent theory, we can generalize the effects of advancing and receding air−water interface movements on detachment of deposited colloids. Theoretical analysis shows that the detachment force (surface tension force) is dependent on the combination of the colloid-air−water and glass-air−water contact angles.

■ ASSOCIATED CONTENT

Supporting Information. A table showing colloid removal at different interface velocities and air−water interface

dx.doi.org/10.1021/la201840q |*Langmuir* 2011, 27, 9985–9993

stages, including the results of the statistical significance tests. This material is available free of charge via the Internet at http://pubs.acs.org.

AUTHOR INFORMATION

Corresponding Author

*Markus Flury. Department of Crop and Soil Sciences, Washington State University, Pullman, WA 99164-6420. Phone: 1-253-445-4522. E-mail: flury@wsu.edu.

ACKNOWLEDGMENT

This material is based upon work supported by the U.S. Department of Energy, Office of Science (BER), under Award No. DE-FG02-08ER64660. We thank the WSU Franceschi Microscopy Center for access to their facility and Chris Davitt for help with the use of the confocal microscope.

REFERENCES

(1) Barthlott, W.; Neinhuis, C. *Phys. Today* **1997**, *202*, 1–8.
(2) Zhang, J.; Sheng, X.; Jiang, L. *Langmuir* **2009**, *25*, 1371–1376.
(3) Neinhuis, C.; Barthlott, W. *Ann. Bot.* **1997**, *79*, 667–677.
(4) Koch, K.; Neinhuis, C.; Ensikat, H. J.; Barthlott, W. *J. Exp. Bot.* **2004**, *55*, 711–718.
(5) Fürstner, R.; Barthlott, W.; Neinhuis, C.; Walzel, P. *Langmuir* **2005**, *21*, 956–961.
(6) Leenaars, A. F. M.; O'Brien, S. B. G. *Philips J. Res.* **1989**, *44*, 183–209.
(7) Dai, Z.; Fornasiero, D.; Ralston, J. *J. Colloid Interface Sci.* **1999**, *217*, 70–76.
(8) Min, Q.; Duan, Y.; Peng, X.; Mujumdar, A. S.; Hsu, C.; Lee, D. *Drying Technol.* **2008**, *26*, 985–995.
(9) Zhuang, J.; McCarthy, J. F.; Tyner, J. S.; Perfect, E.; Flury, M. *Environ. Sci. Technol.* **2007**, *41*, 3199–3204.
(10) Shang, J.; Flury, M.; Chen, G.; Zhuang, J. *Water Resour. Res.* **2008**, *44*, W06411, doi:10.1029/2007WR006516.
(11) Sharma, P.; Abdou, H.; Flury, M. *Vadose Zone J.* **2008**, *7*, 930–940.
(12) McCarthy, J. F.; Zachara, J. M. *Environ. Sci. Technol.* **1989**, *23*, 496–504.
(13) Kretzschmar, R.; Borkovec, M.; Grolimund, D.; Elimelech, M. *Adv. Agron.* **1999**, *66*, 121–193.
(14) Flury, M.; Mathison, J. B.; Harsh, J. B. *Environ. Sci. Technol.* **2002**, *36*, 5335–5341.
(15) Huh, C.; Mason, S. G. *J. Colloid Interface Sci.* **1974**, *47*, 271–289.
(16) Pitois, O.; Chateau, X. *Langmuir* **2002**, *18*, 9751–9756.
(17) Shang, J.; Flury, M.; Deng, Y. *Water Resour. Res.* **2009**, *45*, W06420, doi:10.1029/2008WR007384.
(18) Noordmans, J.; Wit, P. J.; van der Mei, H. C.; Busscher, H. J. *J. Adhesion Sci. Technol.* **1997**, *11*, 957–969.
(19) Gomez-Suarez, C.; Noordmans, J.; van der Mei, H. C.; Busscher, H. J. *Langmuir* **1999**, *15*, 5123–5127.
(20) Gomez-Suarez, C.; Noordmans, J.; van der Mei, H. C.; Busscher, H. J. *Phys. Chem. Chem. Phys.* **1999**, *1*, 4423–4427.
(21) Gomez-Suarez, C.; van der Mei, H. C.; Busscher, H. J. *J. Adhes. Sci. Technol.* **2000**, *14*, 1527–1537.
(22) Gomez-Suarez, C.; Noordmans, J.; van der Mei, H. C.; Busscher, H. J. *Colloids Surf.* **2001**, *186*, 211–219.
(23) Sharma, P.; Flury, M.; Zhou, J. *J. Colloid Interface Sci.* **2008**, *326*, 143–150.
(24) Saiers, J. E.; Lenhart, J. J. *Water Resour. Res.* **2003**, *39*, 1019, doi:10.1029/2002WR001370.
(25) Saiers, J. E.; Hornberger, G. M.; Grower, D. B.; Herman, J. S. *Geophys. Res. Lett.* **2003**, *30*, 2083, doi:10.1029/2003GL018418.
(26) Cheng, T.; Saiers, J. E. *Water Resour. Res.* **2009**, *45*, W08414, doi: 10.1029/2008WR007494.
(27) Hunter, R. J. *Zeta Potential in Colloid Science*; Academic Press: London, 1981.
(28) Shang, J.; Flury, M.; Harsh, J. B.; Zollars, R. L. *J. Colloid Interface Sci.* **2008**, *328*, 299–307.
(29) Decker, E. L.; Frank, B.; Suo, Y.; Garoff, S *Colloids Surf. Physicochem. Eng. Aspects* **1999**, *156*, 177–189.
(30) Lazouskaya, V.; Jin, Y.; Or, D. *J. Colloid Interface Sci.* **2006**, *303*, 171–184.
(31) NIH, *ImageJ*; National Institute of Healths: on-line at http//rsb.info.nih.gov/ij, accessed in June, 2010, 1999.
(32) Haines, W. B. *J. Agric. Sci.* **1930**, *20*, 97–116.
(33) Morrow, N. R. *Ind. Eng. Chem.* **1970**, *62*, 32–56.
(34) Gauglitz, P. A.; Laurent, C. M. S.; Radke, C. J. *Ind. Eng. Chem.* **1988**, *27*, 1282–1291.
(35) Gauglitz, P. A.; Radke, C. J. *AIChE J.* **1989**, *35*, 230–240.
(36) SAS Institute Inc., *SAS/STAT User's Guide, Vers. 6*, 4th ed.; SAS Institute Inc.: Cary, NC, 1990; Vol. 2.
(37) Scheludko, A.; Toshev, B. V.; Bojadjiev, D. T. *J. Chem. Soc., Faraday Trans. I* **1976**, *72*, 2815–2828.
(38) Preuss, M.; Butt, H. *Langmuir* **1998**, *14*, 3164–3174.
(39) Sharma, M. S.; Chamoun, H.; Sita Rama Sarma, D. S. H.; Schechter, R. S. *J. Colloid Interface Sci.* **1992**, *149*, 121–134.
(40) Bretherton, F. P. *J. Fluid Mech.* **1961**, *10*, 166–188.
(41) Nguyen, A.; Schulze, H. *Colloidal Science of Flotation*; Marcel Dekker: New York, 2004.
(42) Schulze, H. *Miner. Process. Extract. Met. Rev.* **1989**, *5*, 43–76.
(43) Albijanic, B.; Ozdemir, O.; Nguyen, A.; Bradshaw, D. *Adv. Colloid Interface Sci.* **2010**, *159*, 1–21.
(44) Song, L.; Johnson, P. R.; Elimelech, M. *Environ. Sci. Technol.* **1994**, *28*, 1164–1171.
(45) Ryan, J. N.; Elimelech, M. *Colloids Surf. Physicochem. Eng. Aspects* **1996**, *107*, 1–56.
(46) Wit, P. J.; Busscher, H. J. *J. Colloid Interface Sci.* **1998**, *208*, 351–352.
(47) Weronski, P.; Elimelech, M. *J. Colloid Interface Sci.* **2008**, *319*, 406–415.